Progress In Electromagnetics Research B, Vol. 28, 1–18, 2011

HYBRID OF PARTICLE SWARM OPTIMIZATION, SIMULATED ANNEALING AND TABU SEARCH FOR THE RECONSTRUCTION OF TWO-DIMENSIONAL TARGETS FROM LABORATORY-CONTROLLED DATA

B. Mhamdi, K. Grayaa, and T. Aguili

Communication Systems Laboratory
Engineer School of Tunis, Belvedere BP 37, Tunis 1002, Tunisia

Abstract—Recently, the use of the particle swarm optimization (PSO) technique for the reconstruction of microwave images has received increasing interest from the optimization community due to its simplicity in implementation and its inexpensive computational overhead. However, the basic PSO algorithm is easily trapping into local minimum and may lead to the premature convergence. When a local optimal solution is reached with PSO, all particles gather around it, and escaping from this local optima becomes difficult. To overcome the premature convergence of PSO, we propose a new hybrid algorithm of particle swarm optimization (PSO), simulated annealing (SA) and tabu search algorithm (TS) for solving the scattering inverse problem. The incorporation of tabu search (TS) and simulated annealing (SA) as local improvement approaches enable the hybrid algorithm to overleap local optima and intensify its search ability in local regions. Reconstructions of dielectric scatterers from experimental inverse-scattering data are finally presented to demonstrate the accuracy and efficiency of the hybrid technique.

1. INTRODUCTION

The objective of microwave imaging is to reconstruct the geometrical and/or physical properties of unknown objects belonging to an inaccessible domain and probed by a set of known incident microwaves. This is performed from measurements of the field scattered by the object under various conditions of illumination. Microwave

Received 29 November 2010, Accepted 4 January 2011, Scheduled 17 January 2011
Corresponding author: Bouzid Mhamdi (bouzid.mhamdi@isetgf.rnu.tn).

tomography has shown great potential in several application areas, notably biomedical imaging [1–3], non destructive testing [4–6], imaging of buried objects and geosciences [7–9]. Certainly, one of the most challenging tasks in defining a microwave-imaging method is to implement a reliable numerical procedure for the inversion of scattered data. In this framework, microwave imaging techniques have been widely investigated in recent years, but they have some intrinsic drawbacks related to the nature of the inverse scattering problems and to the complexity of the hardware setup required to collect the necessary field measures. It is well known that the exact inverse electromagnetic scattering problem, i.e., the quantitative reconstruction of the complex permittivity of a scatterer from measurements of the scattered field for a number of known incident fields is ill-posed and non linear [10]. The main problem in this respect is instability: in the presence of noise on the data, the reconstructions tend to be very different from the actual permittivity profile. As a result, the non-linear inverse scattering problem is reformulated as an optimization problem and solved by iteratively minimizing a cost function. Differences between methods then come from the nature of the criterion and the type of minimization algorithm. Generally speaking, two main kinds of approaches have been developed. The first is based on gradient search approach such as the Newton-Kantrovitch method [11], modified gradient method [12], Levenberg-Marguart algorithm [13] and contrast source inversion method [14] since these approaches apply the gradient search method to find the extreme of the cost function. In general, during the search of the global minimum, these techniques only converge to the exact solution under certain conditions, otherwise, they may be trapped into a local extreme or even diverge. To bypass the difficulties, global stochastic methods such as the genetic algorithm (GA) and simulated annealing (SA) have become attractive alternatives to reconstruct microwave images [15–17]. The neuronal models were also employed to cure the previously quoted disadvantages [18]. The particle swarm optimization (PSO) technique is a relatively new technique for antennas and microwave communities. It has received a huge attention and popularity due to its algorithmic simplicity and effectiveness for solving design problems such as antenna design [19, 20]. Recently, the application of PSO has been extended to the reconstruction of microwave images and excellent results have been reported in the literature [21–23]. One of the main advantages of PSO over other stochastic optimization methods such as GA or SA, lies in the ease with which it can be tuned and implemented, using only a velocity operator to drive the search through out the hyperspace [24]. Although PSO is a good and fast search algorithm to the reconstruction of microwave images, there are still many complex situations where the PSO has premature convergence and tends to converge to local optima, especially in a complex high dimensional problem space. In the worst case, when the best solution found by the group and the particles are all located at the same local minimum, it is almost impossible, due to the velocity update equation, for particles to fly out and do farther searching.

Besides using meta-heuristics as stand alone approaches for solving hard combinatorial optimization problems, during the last years, the attention of researchers has shifted to consider another type of high level algorithms, namely hybrid algorithms. The rationale behind the hybridization resides in the "*No Free Lunch Theorem*" [25, 26] stating that "all algorithms that search for an extremum of a cost function perform exactly the same, when averaged over all possible cost functions. In particular, if algorithm A outperforms algorithm B on some cost functions, then loosely speaking there must exist exactly as many other functions where B outperforms A". Essentially, the theorem states that there is no any search method for optimization which outperforms all other search methods. All these clearly illustrate the need for hybrid evolutionary approaches where the main task is to optimize the performance of the direct evolutionary approach.

Thus, this paper develops a new hybrid technique which combines PSO algorithm with the simulated annealing algorithm (SA) and tabu search (TS) and apply it to solve the scattering inverse problem. SA and TS are powerful optimization procedures that have been successfully applied to a number of combinatorial optimization problems. They have the ability to avoid convergence to local minima. By integrating SA and TS to the PSO, the new algorithm, which we call it PSO-SA-TS can not only escape from local minimum trap in the later phase of convergence, but also simplify the implementation of the algorithm. In other words, PSO contributes to the hybrid approach in a way to ensure that the search converges faster, while the SA and TS make the search to jump out of local optima due to their strong local-search ability. To the best of our knowledge, there is still no investigation on using hybrid technique based on PSO, SA and TS to reconstruct the permittivity profile of dielectric scatterers in free space.

The remaining sections of this paper are organized as follows: Section 2 states the theoretical formulation for the electromagnetic imaging. Section 3 describes the implementations of PSO, SA and TS in the proposed PSO-SA-TS hybrid algorithm. Numerical results for various objects of different permittivity profiles are given in Section 4. Section 5 is the conclusion.

2. PROBLEM FORMULATION

Electromagnetic inversion using optimization techniques is achieved by solving out for the profile which minimizes the error between the observed data and the synthetic one which is obtained by solving the forward problem. The forward problem is introduced first. Let us consider two-dimensional (2-D) geometry as shown in Figure 1.

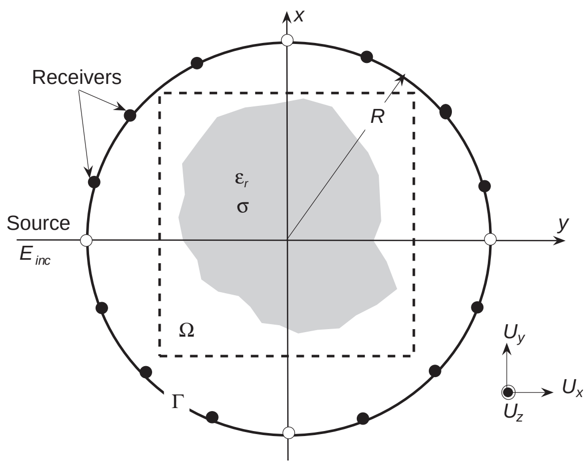

Figure 1. Geometrical configuration of the problem.

A z-oriented cylindrical object of arbitrary cross section in the (x, y) plane is embedded in investigation domain Ω. Only stationary, linear, isotropic and non-dispersive materials are considered. The cylinder is assumed infinite long in z direction, while the cross-section of the cylinder is arbitrary. The material properties of the dielectric scatterer which do not vary along the z-axis are modeled by the contrast function $c(r)$, defined as

$$c(r) = \varepsilon_r(r) - 1 + j\frac{\sigma(r)}{2\Pi f \varepsilon_0} \tag{1}$$

where f indicates the working frequency and ε_0 the dielectric permittivity of the vacuum, while ε_r is the relative dielectric permittivity and σ the electric conductivity. The cylindrical object domain is illuminated by a set of V TM-polarized incident electromagnetic plane waves (since the incident electric field is polarized in the z-axis, ($\vec{e}^{v}_{inc} = e^{v}_{inc}\vec{\mathbf{z}}$). Therefore, the scattering problem is reduced to two dimensional. We assume that the time dependence of the field is harmonic with the factor $\exp(-j\omega t)$. Under these considerations, the scattered field $\vec{e}_s^v = e_s^v \vec{\mathbf{z}}$ and total field $\vec{e}^v = e^v \vec{\mathbf{z}}$ are also parallel to the z-axis considering the scalar nature of the problem. The forward problem which consists of computing the scattered field from the knowledge of the object permittivity profile is solved thanks to a boundary integral equation using the Kirchhoff Helmholtz formula. This leads to two coupled contrast-source integral equations. The first-kind Fredholm integral equation, the so-called observation Equation (2), relates the scattered field e_s^v to Huygens-type sources induced within the target by the incident wave, i.e., to the product of the total field e^v by the contrast (or object) function $c(r)$ representative of the target electromagnetic parameters defined in Ω and null outside:

$$e_s^v(r) = K_0^2 \iint_{\Omega} g(r, r')c(r')e^v(r')dr', \quad r \in \Gamma \tag{2}$$

where, K_0 is the free-space wave number. Γ being the observation domain external to Ω. $g(r, r')$ denotes the two-dimensional Greens function for the background medium. The second Equation (3), denoted as the coupling (or state) equation, is the Lippmann-Schwinger equation. It relates the internal total field e^v in Ω to the induced sources, i.e., to itself and to the contrast c:

$$e^v(r) = e_{inc}^v(r) + K_0^2 \iint_{\Omega} g(r, r')c(r')e^v(r')dr', \quad r \in \Omega \tag{3}$$

In numerical practice, discrete versions of the above equations are considered. The method of moments (MoM) with pulse-basis functions and point matching [27] is then applied to compute the total field e^v for each excitation. The investigation domain Ω under consideration is divided into N homogeneous elementary squares cells. The pixels are selected small enough in order to consider the field and the contrast function as constant over each of them. Once the total field e^v is obtained, secondary quantifies of interest such as the scattered field can be computed. Therefore, (2) and (3) can be transformed into matric equations as follow:

$$E^v = (I - G_\Omega C)^{-1} E_{inc}^v \tag{4}$$

$$E_s^v = G_\Gamma C (I - G_\Omega C)^{-1} E_{inc}^v \tag{5}$$

where E^v and E_{inc}^v are $N \times V$ matrices, theirs v-th columns vectors represent the N elements of the total and incident fields on the test domain Ω correspond to the v-th incidence, respectively. E_s^v is $M \times V$ matrix, its v-th column vector denotes the scattered fields at the M receivers located in measurement domain Γ. G_Ω is $N \times N$ square matrix representing the integrated Greens function in the test domain Ω. G_Γ is $M \times N$ matrix representing the integrated Greens function between

Ω and Γ. I is the identity $N \times N$ matrix, while C is the diagonal $N \times N$ matrix whose elements are the values of contrast at each pixel of Ω.

As it mentioned previously, the resolution of the forward problem consists in determining the scattered field by knowing the object function and the incident field. The computation of inverse solution refers to the procedure of finding the spatial distribution of electromagnetic properties of the scatterer assuming that the permittivity of the embedding medium, the incident field and the values of the measured scattered field at receivers are known. In this study, the scattering inverse problem is reformulated as a nonlinear global optimization problem and is solved by the application of a hybrid particle swarm optimization. By starting from a defined residual as the difference between the calculated scattered field, E_s^v and the measured scattered field, E_{meas}^v. The dielectric permittivity and electric conductivity profiles are determined in an iterative manner in order to minimize a cost functional which gives the normalized deviation between the computed field and the measured field. In the inversion procedure, the hybrid algorithm is used to minimize the following cost function:

$$F(X = [\varepsilon_{r,1}, \varepsilon_{r,2}, \ldots, \varepsilon_{r,N}, \sigma_1, \sigma_2, \ldots, \sigma_N]) = \left(\frac{1}{V} \sum_{v=1}^{V} \frac{\|E_{meas}^v - E_s^v\|^2}{\|E_{meas}^v\|^2} \right)^{\frac{1}{2}} \tag{6}$$

The objective of the optimization inversion algorithm is to find the most suitable vector X which corresponds to the global minimum of the error function given in Equation (6). The value of X which minimizes the error function is supposed to reconstruct the electromagnetic properties profiles close to the original profiles.

3. HYBRID OF PSO, SA AND TS (PSO-SA-TS)

The proposed hybrid algorithm PSO-SA-TS combines PSO with SA and TS. Due to combination of different search mechanisms, not only the PSO operators can keep diversity, but also SA and TS can keep the balance of global search and local search, so the entire search ability of the algorithm can be improved. In this section, PSO, SA and TS are introduced first, followed by a detailed description of PSO-SA-TS.

3.1. Related Algorithms

Particle swarm optimization (PSO) is a population based stochastic optimization technique developed by Kennedy and Eberhart in

1995 [28], inspired by social behavior patterns of organisms. The traditional PSO model consists of a number of particles moving around in the search space. In a space of D dimensions, each particle in the swarm is represented by the following characteristics: $X_i = [X_{i1}, X_{i2}, \ldots, X_{iD}]$: The current position of the particle; $V_i = [V_{i1}, V_{i2}, \ldots, V_{iD}]$: The current velocity of the particle; $P_i = [P_{i1}, P_{i2}, \ldots, P_{iD}]$: The personal best position of the particle. The personal best position of particle i is the best position visited by particle i so far. The position of a particle i is influenced by the local best position P_i visited by itself, i.e., its own experience and the position P_g of the global best particle in the swarm. The performance of each particle is measured using a fitness function that varies depending on the optimization problem. PSO algorithm starts with a group of N_P random (or not) particles (solutions) and then searches for optima by updating each generation. In each iteration, the velocity and position of each particle are updated according to its best encountered position and the best position encountered by any particle, in the following way:

$$\begin{aligned} V_{i,d}(t+1) &= \omega V_{i,d}(t) + c_1 r_1 (P_{i,d}(t) - X_{i,d}(t)) \\ &\quad + c_2 r_2 (P_{g,d}(t) - X_{i,d}(t)) \qquad (7) \\ X_{i,d}(t+1) &= V_{i,d}(t+1) + X_{i,d}(t) \qquad (8) \end{aligned}$$

where ω is the inertia weight. c_1 and c_2 are the acceleration coefficients and the parameters r_1 and r_2 are two random numbers distributed uniformly in $[0, 1]$. ω dynamically reduces during a run which facilitates a balance in the exploration and exploitation of the search space.

Concerning the Simulated annealing algorithm(SA), it was proposed by Kirkpatrik et al. in 1983 [29]. It was one of the first minimization stochastic methods applied to electromagnetic imaging [17]. SA is a probabilistic variant of the local search method, but it can, in contrast, escape local optima. A standard SA procedure begins by generating an initial solution at random. At initial stages, a small random change is made in the current solution X_c. Then the objective function (representing the cost functional F) value of the new solution X_n is calculated and compared with that of the current solution. The probability p of accepting a new solution which called Metropolis law is given as follows:

$$p = \begin{cases} 1, & \text{if} \quad F(X_n) < F(X_c), \\ \exp\left(\frac{-|F(X_n - F(X_c|}{T}\right), & \text{otherwise} \end{cases}, \qquad (9)$$

The calculation of this probability relies on a parameter T, which is referred to as temperature, since it plays a similar role as the temperature in the physical annealing process. To avoid getting trapped at a local minimum point, the rate of T reduction should be slow. In our case, T decrease as follow:

$$T(n+1) = \beta T(n) \tag{10}$$

where the annealing rate satisfies $0 < \beta < 1$.

In this paper, the initial temperature is determined by the following empirical formula:

$$T_0 = -\frac{F_{\max} - F_{\min}}{\ln 0.1} \tag{11}$$

where $F_{\max}$ and $F_{\min}$ denote the maximum and minimum objective values of the solutions in the initial swarm, respectively.

Thus, at the start of SA most worsening moves may be accepted, but at the end only improving ones are likely to be allowed. This can help the procedure jump out of a local minimum.

As a third algorithm, it is the Tabu search (TS) was invented by Glover in 1986 [30], and has been used to solve a wide range of hard optimization problems. TS starts with a random solution and evaluate the fitness function for the given solution. Then all possible neighbors of the given solution are generated and evaluated. TS has two main features: (1) the capability to avoid local optimization. TS uses a tabu list (TL) to memory the better local neighbors which have been searched and will be neglected; (2) the capability to find better resolution. TS uses an aspiration rule to exploit a prohibited resolution. During a situation that all the resolution in the TL is prohibited, the aspiration can make the whole search processing continue. In this work, the following aspiration criterion was employed when all available moves are classified tabu: a tabu move that loses its tabu status by the least increase in the value of current iteration is freed from the tabu list.

3.2. The Proposed PSO-SA-TS Hybrid Approach

In PSO algorithm, particles always chase the current overall optimal point and history optimal point found heretofore [31]. Then the particle speed closes to 0 quickly and can not escape from local minimum. In order to avoid earliness convergence, the algorithm must escape from local minimum and search in other solution space, until solve overall optimal solution. SA and TS algorithms accept a worse solution, it has the ability of escaping from local optimal solution and can restrain earliness convergence, increase the diversity of PSO. The new developed hybrid technique, called PSO-SA-TS, consists in a strong cooperation of PSO, SA and TS, since it maintains the integration of the three techniques for the entire run. The proposed hybrid algorithm makes full use of the exploration ability of PSO and the exploitation ability of SA and TS and offsets the weaknesses of each other. Consequently, through introducing SA and TS to PSO, PSO-SA-TS is capable of escaping from a local optimum. The algorithm starts with a population of particles generated randomly and every particle X_i searches its local best $X_{i,lbest}$ using SA or TS algorithms to update individual personal best P_i and the global P_g. The particles are then subjected to PSO for further refinement. The PSO algorithm handles the global search for the solution while SA and TS facilitates the local search. The driving parameter of the PSO-SA-TS algorithm is the hybridization coefficient (HC) beteween SA and TS; it expresses the percentage of population that in each iteration is evolved with SA: so $HC = 0$ means the procedure is a pure TS (the whole population is updated according to TS operators), $HC = 1$ means pure SA, while $0 < HC < 1$ means that the corresponding percentage of the population is developed by SA, the rest with TS. So, for $HC = 0$ the hybridization is carried out only between PSO and TS and the algorithm will be named PSO-TS. If $HC = 1$, the hybridization is carried out only between PSO and SA and the algorithm will be named PSO-SA. The steps of PSO-SA-TS are given below:

Step 1: Randomly initialize the population of N_p particles within the variable constraint range.

Step 2: Evaluate each particle in the population from the fitness function F.

Step 3:

- Select randomly the particles in population that are evolved with SA.
- Every selected particle X_i generates a new neighbor X'_i in its local area and then according to the accepting rule of SA decides whether to accept the new solution or not. After L iterations, every particle finds its local best solution $X_{i,lbest}$.
- Calculate the new temperature T specified in Equation (10).

Step 4:

- The rest of the population is evolved with TS. Every particle finds its local best solution $X_{i,lbest}$ by applying a TS procedure.
- Update the tabu list (TL).

Step 5: Update personal best P_i and the global best P_g. For each particle, the adaptive fitness value $F(X_{i,lbest})$ is compared with one of the historical best position P_i, if the adaptive value is better than one of P_i. Then, $X_{i,lbest}$ is consider as the best position P_i, otherwise, P_i

remain unchanged.

$$P_i = \begin{cases} X_{i,lbest}, & \text{if} \quad F(X_{i,lbest}) < F(P_i), \\ P_i, & \text{otherwise} \end{cases}, \tag{12}$$

After updating every particles personal best value, we can get the new global best value P_g.

Step 6: Update the position and velocity of each particle by PSO operators according to (7) and (8).

Step 7: Repeat Steps 2–6 until a stopping criterion, such as a sufficiently good solution being discovered or a maximum number of generations being completed, is satisfied.

4. NUMERICAL RESULTS

In this section, we discuss reconstruction results using experimental data. We illustrate the performance of the proposed inversion hybrid algorithm and its sensitivity to random noise in the scattered field. The hybrid algorithm is applied to two different dielectric objects embedded in the free space. The experimental setup under consideration, from Institut Fresnel (Marseille, France), and the experimental data used to test the retrieval algorithm are described in [32]. For these objects, time harmonic multi-frequency and multi-bistatic data are measured at 241 measurement points ($M = 241$) on a circle with a radius R of 1.67 m and for different emitter positions on a circle with a same radius around the target. Relative to a fixed emitting antenna at 0, the receiving antenna is rotated in a limited angular range from 60 to 300 with a 1 stepping. For all the reconstructions, we exploited the experimental data witch corresponding to the frequency 4 GHz. The investigation domain Ω of $0.15 \times 0.15\text{m}^2$ inside is partitioned into 20×20 ($N = 400$) square cells.

As far as the PSO-based method for the retrieval process is concerned, the following configuration of parameters has been adopted according to the guidelines in the related literature [33, 34] and to the heuristic study carried out in [35]. The size of population N_P and the maximum iteration Nmax are set to 300 and 400, respectively. The cognitive coefficients c_1 and c_2 represent the weightings that pull each particle toward p_{best} and g_{best}. Low values let particles wander around their local neighborhood, while high values cause particles to fly toward, or pass, optimal solutions [28]. Thus, we have set $c_1 = c_2 = 2$ suggested by [33] and [34] for the sake of convergence. To further accelerate the convergence, a time-varying inertial weight, ω, is utilized and varies from 0.9 at the beginning to 0.4 toward the end of the optimization [35]. Therefore, in each iteration i, ω is set to

$0.9 - i \times (0.9 - 0.4)/\text{Nmax}$. For the TS algorithm, TL is an essential component, and stores points where the last label positions have been changed. In some applications a simple choice of TL size in a range centered around 7 seems to be quite effective [36]. In our case, the TL size is set to 5. The temperature decrement cooling factor β is set to a constant value of 0.9.

To evaluate the quality of the reconstructions, a relative error ξ_{ε_r} of dielectric permittivity between the reconstructed profile and the original one is defined as:

$$\xi_{\varepsilon_r} = \left(\frac{1}{N} \sum_{n=1}^{N} \frac{|\varepsilon_{r,n}^{true} - \varepsilon_{r,n}^{cal}|^2}{|\varepsilon_{r,n}^{true}|^2} \right)^{\frac{1}{2}} \tag{13}$$

where the superscript cal and true stand for the reconstructed profile and the true one, respectively.

In what follows, some reconstructions using the experimental data are presented.

The first object consists of two purely dielectric targets: the first target is a foam cylinder of diameter = 80 mm, its relative permittivity was estimated to be $\varepsilon_r = 1.45 \pm 0.15$. The second target is a plastic cylinder of diameter = 31 mm, its relative permittivity was estimated to be $\varepsilon_r = 3 \pm 0.3$. The dielectric cylinders being close together (see [32] for more details on the experimental setup, in which the target under test is referred therein as **FoamDielExt**).

Before performing further numerical assessments with different test examples, it is worth analyzing the impact of the choice of hybridization coefficient HC. Toward this aim, several reconstructions of the first object have been performed. Figure 2 shows the variation of the permittivity error ξ_{ε_r} according to HC parameter. It is quite

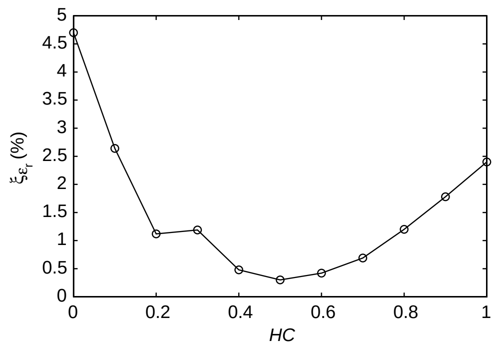

Figure 2. The permittivity error ξ_{ε_r} vs. hybridization coefficient HC.

clear that ξ_{ε_r} is minimal for HC values close to 0.5. Consequently, 0.5 will be selected as optimal value of HC and the employment of PSO-SA-TS will indicate implicitly that $HC = 0.5$.

The reconstructed profiles using the standard PSO and the others three versions of hybrid algorithms (PS0-TS, PSO-SA and PSO-SA-TS) are shown in Figure 3. It is quite remarkable that the reconstructions are close to the exact original profile of the **FoamDielExt** object. However, it is clear that the best reconstructing quality is obtained by the new hybrid algorithm PSO-SA-TS, indeed the permittivity error ξ_{ε_r} is of 0.105, 0.047, 0.024 and 0.003 for PSO, PSO-TS, PSO-SA and PSO-SA-TS, respectively. The convergence status of the cost functional F for different generations corresponding to the best particle in the swarm is shown in Figure 4. It is evident from this figure that the hybridization of PSO, SA and TS has much better effect on the speed of convergence.

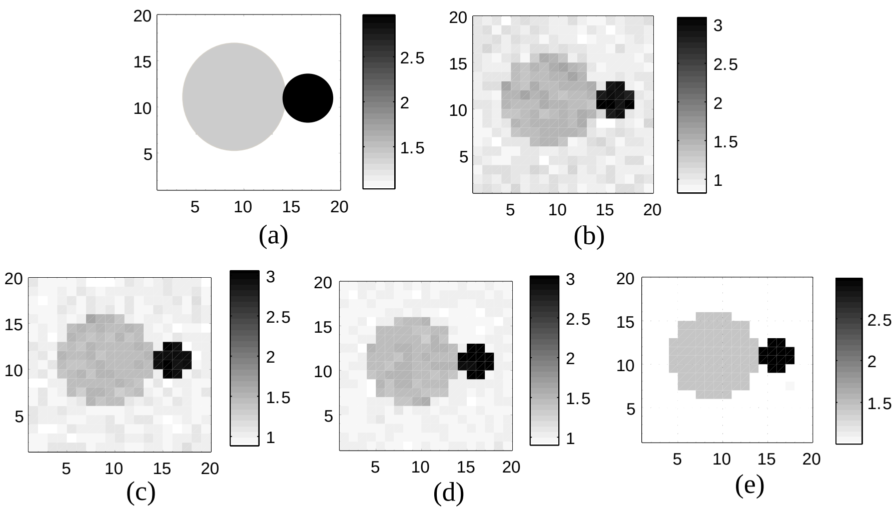

Figure 3. Reconstructions of the **FoamDielExt**. (a) Original object. (b) Reconstruction using standard PSO. Reconstruction for different value of HC, (c) $HC = 0$, (d) $HC = 1$ and (e) $HC = 0.5$.

The conductivity profile was found more or less homogeneous inside the search domain and close to zero. Therefore, it is not presented.

As a second example, we considered an object consisted of two plastic cylinders and a Foam cylinder which have the same characteristics as those of the first example but placed in a different configuration. The experimental data are fully described in [32] and the target is referred therein as **FoamTwinDiel**. The gray-level representations of the retrieved profiles as well as a cut of these profiles in the object medium along the x axis are reported in Figures 5 and 6, respectively. If we compare Figure 5(b) with Figure 5(c), the latter provides a clear estimate of the shape of the **FoamTwinDiel** object as well as of the inhomogeneity of this scatterer.

In the final generation, the permittivity error ξ_{ε_r} is about 5.62 and 0.64 for PSO and PSO-SA-TS, respectively. We note that the reconstructed profiles of the conductivity which are not represented here are almost found homogenous and practically tend towards zero.

A significant performance criterion of an optimization algorithm is the computing times. The inversion using standard PSO and PSO-SA-TS takes 72 minutes 23 seconds and 26 minutes 43 seconds, respectively.

In order to investigate the robustness of the imaging algorithm against random noise, an additive white Gaussian noise of zero mean is added into the experimental electric fields. Several values of the signal to noise ratio (SNR) are used to reconstruct **FoamTwinDiel**.

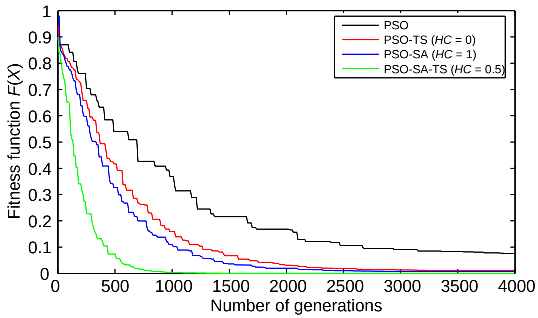

Figure 4. Fitness function F at different generations in inversion of **FoamDielExt** using both hybrid algorithms and standard PSO.

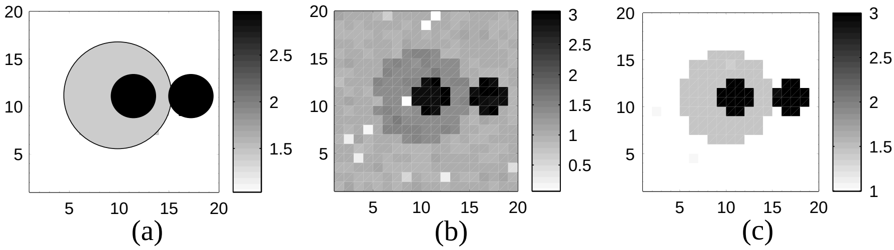

Figure 5. Reconstructions of **FoamTwinDiel**. (a) Original object. Reconstruction using: (b) Standard PSO, (c) PSO-SA-TS.

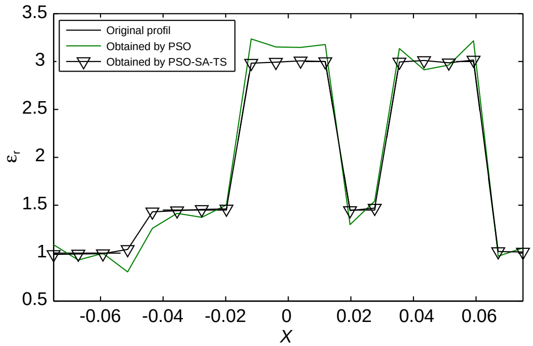

Figure 6. Permittivity profiles of **FoamTwinDiel** along the x axis.

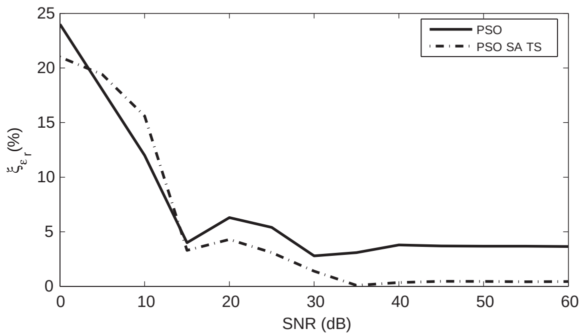

Figure 7. Effect of noise.

Figure 7 shows the effect of random noise on PSO and PSO-SA-TS for reconstructing the second example. From this figure, one concludes that the hybrid algorithm is much more robust against noise than the standard PSO.

Comparing the obtained simulation results by PSO-SA-TS with those obtained by classic PSO, it is found that the PSO-SA-TS shows a much higher level of robustness than standard PSO.

5. CONCLUSION

In this study, we have proposed a new optimization technique based on the hybridization of the Particle Swarm Optimization with the Simulated Annealing and Tabu Search to solve an inverse scattering problem from laboratory-controlled data. The forward problem is computed using the method of moments.

The inverse problem is reformulated in to an optimization one, and then the global searching scheme PSO-SA-TS is employed to reconstruct the dielectric targets from experimental data. The comparisons with standard PSO, demonstrate the superiority of PSO-SA-TS in higher convergence accuracy and fewer cost function evaluations. Numerical results have been carried out and good reconstruction has been obtained even in the presence of additive white Gaussian noise in experimental data. Future work will involve evaluating the algorithm using 3D simulations and using an experimental data.

REFERENCES

1. Zhou, H., T. Takenaka, J. Johnson, and T. Tanaka, "A breast imaging model using microwaves and a time domain three dimensional reconstruction method," *Progress In Electromagnetics Research*, Vol. 93, 57–70, 2009.
2. Zhang, H., S. Y. Tan, and H. S. Tan, "A novel method for microwave breast cancer detection," *Progress In Electromagnetics Research*, Vol. 83, 413–434, 2008.
3. Guo, B., Y. Wang, J. Li, P. Stoica, and R. Wu, "Microwave imaging via adaptive beamforming methods for breast cancer detection," *Journal of Electromagnetic Waves and Applications*, Vol. 20, No. 1, 53–63, 2006.
4. Kharkovsky, S. and R. Zoughi, "Microwave and millimeter wave nondestructive testing and evaluation — overview and recent advances," *IEEE Instrum. and Meas. Mag.*, Vol. 10, 26–38, Apr. 2007.
5. Thomas, V., J. Yohannan, A. Lonappan, G. Bindu, and K. T. Mathew, "Localization of the investigation domain in electromagnetic imaging of buried 2-D dielectric pipelines with circular cross section," *Progress In Electromagnetics Research*, Vol. 61, 111–131, 2006.
6. Benedetti, M., M. Donelli, G. Franceschini, M. Pastorino, and A. Massa, "Effective exploitation of the a-priori information through a microwave imaging procedure based on the SMWfor NDE/NDT applications," *IEEE Trans. Geosci. Remote Sens.*, Vol. 43, No. 11, 2584–2592, Nov. 2005.
7. Zhang, Z. Q. and Q. H. Liu, "Applications of the BiCGS-FFT method to 3-D induction well logging problems," *IEEE Geosci. Remote Sensing*, Vol. 41, 856–869, May 2003.
8. Catapano, I., L. Crocco, R. Persico, M. Pieraccini, and

F. Soldovieri, "Linear and nonlinear microwave tomography approaches for subsurface prospecting: Validation on real data," *IEEE Antennas Wireless Propag. Lett.*, Vol. 5, 49–53, Dec. 2006.

9. Crocco, L., M. D'Urso, and T. Isernia, "The contrast source-extended born model for 2D subsurface scattering problems," *Progress In Electromagnetics Research B*, Vol. 17, 343–359, 2009.
10. Hofmann, B. and O. Scherzer, "Factors influencing the illposedness of nonlinear problems," *Inverse Problems*, Vol. 10, 1277–1297, 1994.
11. Qing, A. and L. Jen, "A novel method for microwave imaging of dielectric cylinder in layered media," *Journal of Electromagnetic Waves and Applications*, Vol. 11, No. 10, 1337–1348, 1997.
12. Van Den Berg, P. M. and M. van der Horst, "Nonlinear inversion in induction logging using the modified gradient method," *Radio Sci.*, Vol. 30, 1355–1369, 1995.
13. Hettlich, F., "Two methods for solving an inverse conductive scattering problem," *Inverse Problems*, Vol. 10, 375–385, 1994.
14. Van Den Berg, P. M. and R. E. Kleinman, "A contrast source inversion method," *Inverse Problems*, Vol. 13, 1607–1620, 1997.
15. C.-L., Liu, C.-C. Chiu, T.-C. Tu, and M.-F. Tasi, "Electromagnetic transverse electric-wave inverse scattering of an imperfectly conducting cylinder by genetic algorithms," *Journal of Microwaves, Optoelectronics and Electromagnetic Applications*, Vol. 7, 1–15, Jun. 2008.
16. Chien, W., "Inverse scattering of an un-uniform conductivity scatterer buried in a three-layer structure," *Progress In Electromagnetics Research*, Vol. 82, 1–18, 2008.
17. Garnero, L., A. Franchois, J. P. Hugonin, C. Pichot, and N. Joachimowicz, "Microwave imaging-complex permittivity reconstruction-by simulated annealing," *IEEE Trans. Microw. Theory Tech.*, Vol. 39, 1801–1807, 1991.
18. Brovko Alexander, V., K. Murphy Ethan, and V. Yakovlev Vadim, "Waveguide microwave imaging: Neural network reconstruction of functional 2-D permittivity profiles," *IEEE Trans. Microw. Theory Tech.*, Vol. 57, No. 2, Feb. 2009.
19. Boeringer, D. W. and D. H. Werner, "Particle swarm optimization versus genetic algorithms for phased array synthesis," *IEEE Trans. Antennas Propagat.*, Vol. 52, 771–779, Mar. 2004.
20. Li, W.-T., X.-W. Shi, and Y.-Q. Hei, "An improved particle swarm optimization algorithm for pattern synthesis of phased arrays," *Progress In Electromagnetics Research*, Vol. 82, 319–332, 2008.

21. Huang, C.-H., C.-C. Chiu, C.-L. Li, and K.-C. Chen, "Time domain inverse scattering of a two-dimensional homogenous dielectric object with arbitrary shape by particle swarm optimization," *Progress In Electromagnetics Research*, Vol. 82, 381–400, 2008.
22. Donelli, M., D. Franceschini, P. Rocca, and A. Massa, "Three dimensional microwave imaging problems solved through an efficient multiscaling particle swarm optimization," *IEEE Geoscience and Remote Sensing*, Vol. 47, 1467–1481, 2009.
23. Emad Eldin, A. M., E. A. Hashish, and M. I. Hassan, "Inversion of lossy dielectric profiles using particle swarm optimization," *Progress In Electromagnetics Research M*, Vol. 9, 93–105, 2009.
24. Kennedy, J. and R. C. Eberhart, *Swarm Intelligence*, Morgan Kaufmann, San Francisco, 2001.
25. Wolpert, D. H. and W. G. Macready, "No free lunch theorems for optimization," *IEEE Trans. Evolutionary Comp.*, Vol. 1, 67–82, 1997.
26. Fulginei, F. R. and A. Salvini, "Comparative analysis between modern heuristics and hybrid algorithms," *COMPEL: Int. Journal for Comp. and Mathematics in Electrical and Electronic Engineering*, Vol. 26, 259–268, 2007.
27. Harrignton, R. F., *Field Computation by Moments Methods*, IEEE Press, Piscataway, NJ, 1993.
28. Kennedy, J. and R. C. Eberhart, "Particle swarm optimization," *Proc. IEEE International Conference on Neural Networks*, Vol. 4, 1942–1948, IEEE Service Center, Piscataway, 1995.
29. Kirkpatrick, S., C. D. Gelatt, Jr. and M. P. Vecchi, "Optimization by simulated annealing," *Journal of Science*, Vol. 220, 671–680, 1983.
30. Glover, F., "Tabu search: Part 1," *ORSA Journal on Computing*, Vol. 1, No. 3, 190–206, 1989.
31. Pan, H. and X. Han, "BP network learning algorithm research and application of PSO algorithm," *Computer Engineering and Application*, Vol. 44, No. 9, 67–69, 2008.
32. Geffrin, J.-M., P. Sabouroux, and C. Eyraud, "Free space experimental scattering database continuation: Experimental set-up and measurement precision," *Inverse Problems*, Vol. 21, 117–130, 2005.
33. Jin, N. and Y. Rahmat-Samii, "Advances in particle swarm optimization for antenna designs: Real-number, binary, single-objective and multiobjective implementations," *IEEE Transac-*

tions on Antennas and Propagation, Vol. 55, 556–567, 2007.

34. Robinson, J. and Y. Rahmat-Samii, "Particle swarm optimization in electromagnetics," *IEEE Transactions on Antennas and Propagation*, Vol. 52, 771–778, 2004.
35. Caorsi, S., M. Donelli, D. Franceschini, and A. Massa, "A new methodology based on an iterative multiscaling for microwave imaging," *IEEE Trans. on Microwave Theory Tech.*, Vol. 51, 1162–1173, 2003.
36. Sudhakaran, M. and P. Ajay-D-Vimal Raj, "Integrating genetic algorithms and tabu search for unit commitment problem," *International Journal of Engineering, Science and Technology*, Vol. 2, 57–69, 2010.